1-D Magnetotelluric (MT) Inversion with Spatial Constraint:
A Comparison to 3-D Resistivity Model from Mae Chan Geothermal System

Submitted June 2020

Dechpinthong Lappanichpoolpol

Advisors
Dr. Puwis Amatyakul

Geophysics Research Group, Department of Physics
Faculty of Science, Mahidol University

June, 2020

ABSTRACT

Magnetotelluric (MT) method is an electromagnetic (EM) geophysical exploration method. This is one of the widely used techniques in the geophysical survey. This method has contributed to many geophysical prospecting including geothermal, hydrocarbon, and mineral explorations e.g. S. Boonchaisuk et al., 2013; P. Amatyakul et al., 2015.

The Earth's electric field and magnetic field at the surface are recorded by stations in the investigation area. The source of these fields is a natural electromagnetic wave propagating downward from the ionosphere and diffuses into Earth's subsurface according to its frequency. The relation between both fields and subsurface resistivity distribution is governed by Maxwell's equations in the frequency domain. By using the inversion software, a kind of advanced mathematical optimization, the resistivity model of the subsurface can be obtained.

There are many available 3-D MT inversion software e.g. W. Siripunvaraporn et al., 2005; W. Siripunvaraporn, and G. Egbert, 2009. Most of the 3-D inversion takes a large computational time to obtain the 3-D resistivity model. It is not practical to obtain the 3-D resistivity model during the field operation. It will be a great benefit to get the estimated resistivity model for the 3-D MT acquisition or called quasi 3-D MT resistivity model.

E. Auken et al., 2005 used 1-D MT inversion to reveal the resistivity structure at the minimal computational time. There is also other work using 1-D MT inversions to estimate the 3-D resistivity model e.g. Fernando Aca´cio Monteiro Santos et al., 2011.

However, the problems with the 1-D MT inversion are giving a rough picture but 3-D MT inversion sharpening the resistivity structure. The 3-D inversion reveals much more consistent details than the 1-D inversion (Charles Muturia Lichoro, 2015). Therefore, we propose to develop an efficient 1-D MT inversion by taking structural information between MT sites simultaneously during the inversion process.

Keywords: Magnetotelluric method, geophysical prospecting, MT inversion, spatial constraint

ACKNOWLEDGEMENTS

I would like to thank Dr. Puwis Amatyakul for the kind support and advice. I would like to thank people in the geophysics research group at Mahidol University for their support and the information for my research.

Finally, I also thank Mahidol University for supporting MATLAB license, which is the main program for my project.

CONTENTS

CONTENTS (Cont.)

LIST OF FIGURES

LIST OF FIGURES (Cont.)

Figures **Page**

CHAPTER I

INTRODUCTION

In the present world, most useful natural resources can be obtained from underground. The excavation cost is dramatically increased following the deepness of the hole, according to this reason, the scientific suggestion is very important in order to assure the location of resources. The Magnetotelluric (MT) method is an electromagnetic (EM) geophysical exploration method. This is one of the widely used techniques in the geophysical survey. This method has contributed many geophysical prospecting including geothermal, hydrocarbon, and mineral explorations.

1.1 Motivation

Most of the 3-D inversion takes a large computational time to obtain the 3-D resistivity model. It is not practical to obtain the 3-D resistivity model during the field operation. It will be a great benefit to get the estimated resistivity model for the 3-D MT acquisition or called quasi 3-D MT resistivity model. Therefore, we propose to develop an efficient 1-D MT inversion by taking structural information between MT sites simultaneously during the inversion process.

1.2 Aims and Objectives

This work aims to develop an efficient 1-D MT inversion estimating resistivity model for 3-D MT or called spatially-constrained 1-D MT inversion. This will enable getting accurate quasi 3-D resistivity structure by using this newly develop 1-D MT inversion.

1.3 Modeling

Modeling is an important procedure for determining the model of the subsurface from the data response by the associated governing physics principles. There are two essential parts of geophysical modeling, forward modeling and inversion.

1.3.1 Forward Modeling

Forward modeling is a process which calculates the predicted data response of a survey from the known model through theoretical or numerical calculations. In most cases, numerical calculation is required because of the model complexity.

1.3.2 Inversion

For geophysical problems, there is no simple and direct relation to calculate the subsurface model from the measurement data. This can be conducted through a mathematical optimization process called “inversion” which finds the model that fits the input data.

CHAPTER II

BACKGROUND AND RELATED WORKS

2.1 Magnetotellurics: Basic Theoretical Concepts

2.1.1 Introduction

The Magnetotelluric method or Magnetotellurics (MT) is an electromagnetic geophysical exploration technique that images the electrical properties (distribution) of the Earth at subsurface depths. The energy for the Magnetotelluric technique is from natural source of external origin. When this external energy, known as the primary electromagnetic field, reaches the Earth's surface, part of it is reflected back and remaining part penetrates into the Earth. Earth acts as a good conductor, thus electric currents (known as telluric currents) are induced in turn produce a secondary magnetic field.

Magnetotellurics is based on the simultaneous measurement of total electromagnetic field, i.e. time variation of both magnetic field $B(t)$ and induced electric field $E(t)$. The electrical properties (e.g. electrical conductivity) of the underlying material can be determined from the relationship between the components of the measured electric (E) and magnetic field (B) variations, or transfer functions: The horizontal electric (E_x and E_y) and horizontal (B_x and B_y) and vertical (B_z) magnetic field components. According to the property of electromagnetic waves in the conductors, the penetration of electromagnetic wave depends on the oscillation frequency. The frequency of the electromagnetic fields development of the theory determines the depth of penetration.

The basis for MT method is found by Tikhonov (1950) and Cagniard (1953). In half a century since its inception, important developments in formulation, instrumentation and interpretation techniques have yielded MT as a competitive geophysical method, suitable to image broad range of geological targets.

2.1.2 Source Field of MT Signals

The MT signals are generated from two sources:

1. At the lower frequencies, generally less than 1 Hz, or more than 1 cycle per second, the source of the signal is originated from the interaction of the solar wind with the Earth's magnetic field. As solar wind emits streams of ions, it travels into space and disturbs the Earth's ambient magnetic field and produces low-frequency electromagnetic energy that penetrates the Earth.

2. The high frequency signal is greater than 1 Hz or less than 1 cycle per second is created by world-wide thunderstorm activity, usually near the equator. The energy created by these storms travels around the Earth in a wave guide between the Earth's surface and the ionosphere, with part of the energy penetrates into the Earth.

2.1.3 Principles of MT

2.1.3.1 Maxwell's Equation

The electromagnetic fields within a material of a non-accelerated reference frame can be described by Maxwell's equations. These can be expressed in differential form with the International system of Units (SI) as:

$$\nabla \times E = -\frac{\partial B}{\partial t}; \text{ Faraday's law} \tag{2.1}$$

$$\nabla \times H = J + \frac{\partial D}{\partial t}; \text{ Ampere's law} \tag{2.2}$$

$$\nabla \cdot D = \rho_V; \text{ Gauss's law} \tag{2.3}$$

$$\nabla \cdot B = 0; \text{ Gauss's law for magnetism} \tag{2.4}$$

where E (V/m) and H (A/m) are the electric and magnetic fields, B is the magnetic induction. D (C/m^2)) is the displacement current and ρ (C/m^3)) is the electric charge density owing to free charges. J and $\frac{\partial D}{\partial t}$ (A/m^2) are the current density and the varying displacement current respectively.

Maxwell's equations can also be related through their constitutive relationship:

$$J = \sigma E, \tag{2.5}$$

$$D = \varepsilon E, \tag{2.6}$$

$$B = \mu H, \tag{2.7}$$

σ, ε and μ describe intrinsic properties of the materials through which the electromagnetic fields propagate. σ (S/m) is the electrical conductivity (its reciprocal being the electrical resistivity $\rho = 1/\sigma$ (Ω-m)), ε (F/m) is the dielectric permittivity and μ (H/m) is the magnetic permeability. These magnitudes are scalar quantities in isotropic media. In anisotropic materials they must be expressed in a tensorial. In this work, it will be assumed that the properties of the materials are isotropic.

In a vacuum, the dielectric permittivity is $\varepsilon = \varepsilon_0 = 8.85 \times 10^{-12}$ F/m. Within the Earth, this value ranges from ε_0 (vacuum and air) to 80 ε_0 (water). It can also vary depending on the frequency of the electromagnetic fields; Christopherson (1998).

For most of the Earth materials and for the air, the magnetic permeability ''μ'' can be approximated to its value in a vacuum, $\mu_0 = 4\pi \times 10^{-7}$ H/m. However, in highly magnetized materials this value can be greater, for example, due to an increase in the magnetic susceptibility below the Curie point temperature (Hopkinson effect, e.g. Keller (1987)).

Across a discontinuity between two materials, named 1 and 2, the boundary conditions to be applied to the electromagnetic fields and currents described by Maxwell's equations are:

$$\mathrm{n} \times (E_2 - E_1) = 0, \tag{2.8}$$

$$\mathrm{n} \times (H_2 - H_1) = Js, \tag{2.9}$$

$$\mathrm{n} \times (D_2 - D_1) = \rho_s, \tag{2.10}$$

$$\mathrm{n} \times (B_2 - B_1) = 0, \tag{2.11}$$

$$\mathrm{n} \times (J_2 - J_1) = 0, \tag{2.12}$$

where n is the unit vector normal to the discontinuity boundary, Js (A/m2) is the current density along the boundary surface and ρ_s (C/m^2) is the surface charge density. In the absence of surface currents, and considering constant values of ε and μ, the tangential components of E and the normal components of J are continuous, whereas the both tangential and normal components of B are continuous across the discontinuity.

Due to the nature of the electromagnetic sources used in MT, the properties of the Earth materials and the depth of investigations considered, two hypotheses are applicable:

(a) Quasi-stationary approximation: Displacement currents ($\frac{\partial D}{\partial t}$) can be neglected relative to conductivity currents (J) for the period range 10^{-5} to 10^{5} s and for not extremely low conductivity values. Therefore, the propagation of the electromagnetic fields through the Earth can be explained as a diffusive process, which makes it possible to obtain responses that are volumetric averages of the measured Earth conductivities.

(b) Plane wave hypothesis: The primary electromagnetic field is a plane wave that propagates vertically down towards the Earth surface (z direction); Radhakrishnamurthy C, Likhite SD (1970).

The searched solutions of the electromagnetic fields from Maxwell's equation can be expressed through a linear combination of harmonic wave:

$$E = E_0 \cdot e^{i(wt+kr)} \tag{2.13}$$

$$B = B_0 \cdot e^{i(wt+kr)} \tag{2.14}$$

where ω (rad/s) is the angular frequency of the electromagnetic oscillations, t(s) is the time; k(m^{-1}) and r(m) are the wave and position vectors respectively. In both expressions, the first term in the exponent corresponds to wave oscillations and the second term represents wave propagation.

Using the harmonic expressions of the electromagnetic fields (Eqs. 2.13 and 2.14) and their constitutive relationships (Eqs. 2.5–2.7), Maxwell's equations in frequency domain for MT hypothesis (a quasi-stationary approximation) are described as follows:

$$\nabla \times E = -i\omega B \tag{2.15}$$

$$\nabla \times H = \mu_0 \sigma E \tag{2.16}$$

$$\nabla \cdot E = \frac{\rho\varepsilon}{\epsilon} \tag{2.17}$$

$$\nabla \cdot B = 0 \tag{2.18}$$

where the value of the magnetic permeability (μ) is considered equal to the value in a vaccum (μ_0).

In the absence of charges, the right term of Eq. 2.17 vanishes, and the electric and magnetic field solutions depend solely upon angular frequency (ω) and conductivity (σ).

Finally using the hypothesis (b) (plane wave) and applying the boundary conditions (Eqs. 2.8–2.12) across discontinuities, the solutions of Maxwell's equations can be obtained.

In the case of a homogeneous structure, the components of the electric and magnetic fields take the form:

$$Ak = A_{k0} \cdot e^{iwt} \cdot e^{-i\alpha z} \cdot e^{-\alpha z} \tag{2.19}$$

with $\alpha = \sqrt{\mu\sigma\omega/2}$ (m^{-1}) the first factor of the equation is the wave amplitude, the second and third factor (imaginary exponentials) is sinusoidal time and depth variations respectively and the fourth is exponential decay. This decay can be quantified by the skin depth (δ), and the value of z for which this term decays to 1/e; Vozoff K (1972) :

$$\delta = \sqrt{\frac{2}{\mu_0\sigma\omega}} \approx 500\sqrt{\rho T} \text{ (m).} \tag{2.20}$$

The skin depth permits the characterization of the investigation depth, which, as can be seen, increases according to the square root of the product of medium resistivity and period. Although it has been defined for homogeneous media, its use can be extended to heterogeneous cases as well (e.g. geological structures). The above text has been taken from the Telford et al.

2.1.3.2 Uniform Half Space

In this case Earth is treated as a conducting half space with a plane surface. The assumptions usually made about the source field; Cagniard L (1953) are that it is homogeneous, infinite in dimension and is located effectively at infinity so that plane EM waves 18 2 Magnetotellurics: Basic Theoretical Concepts impinging on the Earth surface. Under these conditions, there are no horizontal variations of the EM field, i.e. $\frac{\partial E}{\partial x} = \frac{\partial H}{\partial x} = \frac{\partial E}{\partial y} = \frac{\partial H}{\partial y} = 0$. Hence $H_z = 0 = E_z = 0$ for the X component, Eq. 2.7 reduces to

$$\frac{\partial^2 E_x}{\partial Z^2} = K^2 E_x \tag{2.21}$$

where $K^2 = i\mu\omega\sigma$. From Maxwell's equation,

$$H_y = (-i/\omega\mu)\frac{\partial E_x}{\partial Z} \tag{2.22}$$

Since the fields originate from a source above the earth, all the field quantities must remain finite. At $Z = \infty$. Hence the solution of Eq. 2.21 is

$$E_x = Qe^{-KZ} \tag{2.23}$$

where Q is a constant.

As seen from the foregoing an electromagnetic wave propagating into the earth (linear, homogeneous and isotropic) has its electric and magnetic field wave vectors orthogonal to each other, and the ratio of electric and magnetic field intensity (E/H) termed as the impedance (Z) is a characteristic measure of the EM properties of the sub surface medium, and constitutes the basic MT response function.

For a plane wave, we have

$$Z = \frac{E_x}{H_y} = \frac{i\omega\mu}{k} \tag{2.24}$$

where Z is the characteristic impedance, Ex the electric field intensity (north) in mv/km and H_y the magnetic field intensity (east) in γ (10^{-5} Oe)

$$Z = \sqrt{\frac{i\omega\mu}{\sigma}} \tag{2.25}$$

From the above equation it may be deduced that in a homogeneous and isotropic half-space, the magnetic field lags behind the electric field by $\pi/4$ rad.

The true resistivity of the half-space is

$$\rho = \frac{1}{\sigma} = \frac{|Z|^2}{\mu\omega} = \frac{T}{2\pi\mu}|Z|^2 \tag{2.26}$$

where T is the period, with the EM system of units, Cagniard L (1953) has obtained the following equation as

$$\rho = 0.2T\frac{|E_x|^2}{|H_y|^2} \tag{2.26a}$$

where ρ = resistivity in Ω-m

E = the horizontal electric field in mv/km

H = the orthogonal horizontal magnetic field in gamma and

T = period in seconds

When the earth resistivity is non-uniform, the right hand sides of Eq. 2.26a provide apparent resistivities (ρ_a; instead of true resistivity), which are frequency (period) dependent, as is the case with 1-D, 2-D, or 3-D situations.

In a homogeneous and isotropic earth, the true resistivity of the earth is related to the characteristic impedance ''Z'' through the relation:

$$\rho_a = 0.2T|Z|^2 = 0.2T\frac{|E|^2}{|H|^2} \tag{2.27}$$

Where $Z = E/H$ **Note**: $Z = E/H$

$$Z_{xy} = E_x/H_y$$

$$Z_{yx} = E_y/H_x$$

where ρ_a is the apparent resistivity in Ω -m and T is the period in sec,

and phase of Z_{xy},

$$\varphi = \tan^{-1}\frac{\left(\mathrm{Im}\left[\frac{E_x}{H_y}\right]\right)}{\left(\mathrm{Re}\left[\frac{E_x}{H_y}\right]\right)}. \tag{2.28}$$

CHAPTER III
METHODOLOGY

3.1 Forward Modeling

3.1.1 1-D Forward Modeling

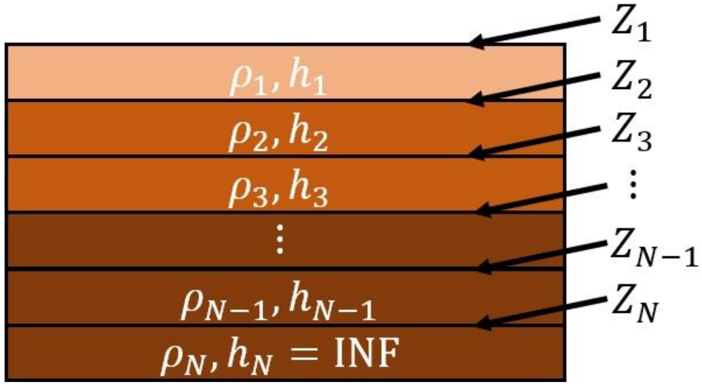

Figure 3.1: 1-D Earth Model

Applying boundary conditions for 1-D or layered medium results in a recursive formula relating impedance of two consecutive layers. So we get the formula to calculate the impedance on surface (Z_1) by

$$Z_{N-1} = Z_{0N-1}\frac{1-R_{N-1}\exp(-2k_{N-1}h_{N-1})}{1+R_{N-1}\exp(-2k_{N-1}h_{N-1})}, \tag{3.1}$$

where $R_{N-1} = \frac{Z_{0N-1}-Z_N}{Z_{0N-1}+Z_N}$; reflection coefficient,

$Z_{0N-1} = (i\omega\mu_0\rho_{N-1})^{1/2}$; intrinsic impedance,

$k_{N-1} = (\frac{i\omega\mu_0}{\rho_{N-1}})^{1/2}$; induction parameter,

$Z_N = Z_{0N} = (i\omega\mu_0\rho_N)^{1/2}$; impedance at N-th (or last) layer.

Then, we can calculate the apparent resistivity

$$\rho_a = \frac{1}{\omega\mu}|Z_1|^2, \tag{3.2}$$

and phase

$$\phi = tan^{-1}\left(\frac{Im\{Z_1\}}{Re\{Z_1\}}\right). \tag{3.3}$$

We plot both of them to different frequencies (f_i) or periods (T_i).

3.1.2 Pseudo Code for Forward Modeling

Import frequencies, resistivities, and thicknesses of each layers

Assign magnetic permeability (μ_0)

for all frequencies

  Calculate angular frequency

  Calculate impedance at the deepest layer

  for before the deepest layer to surface

    Calculate the impedance on surface using recursive formula

  end

  Calculate apparent resistivity

  Calculate phase

end

3.2 Occam's inversion

Occam's inversion was proposed by Constable et al. (1987) for 1-D MT and 1-D schlumberger DCR. The philosophy of the Occam approach is to seek the "smoothest" or "minimum" structure model subject to a constraint on the misfit (see Constable et al., 1987; Siripunvaraporn & Egbert, 2000; Boonchaisuk et al., 2008), which can be mathematically transformed into a problem of minimization of an objective function W,

$$W = \Phi_m + \lambda^{-1}\Phi_d. \tag{3.4}$$

Φ_m denotes the "model function". Φ_d represents the "data functional". Here, we want to minimize Φ_m subject to $\Phi_d = 0$. λ is introduced as the Lagrange multiplier acting as the regularization or trade-off parameter between the model and data functionals.

3.2.1 Data functional

$$\Phi_d = \chi_d^2 - \chi_{d^*}^2, \tag{3.5}$$

As with the least-square problem, χ_d^2 represents an average variance between the measured data (d) and the numerically predicted data (f) which can be expressed by

$$\chi_d^2 = \sum_{i=1}^{N} \left(\frac{d_i - f_i}{\epsilon_i}\right)^2, \tag{3.6}$$

where ϵ_i is the error of the measured data d_i and N is the number of data.

Equation (3.6) can be expressed in matrix form as,

$$\chi_d^2 = (d - \mathrm{F}[m])^{\mathrm{T}} C_d^{-1} (d - \mathrm{F}[m]), \tag{3.7}$$

where d is a vector containing the measured data.

$\mathrm{F}[m]$ is a vector containing the predicted data generated by the forward modeling from the model vector m (F represents the forward modeling operator),

$$\mathrm{F}[m] = \begin{bmatrix} \rho_{a1} \\ \vdots \\ \rho_{aN} \\ \phi_1 \\ \vdots \\ \phi_N \end{bmatrix}_{2N\times 1} \tag{3.8}$$

ρ_1
ρ_2
$\vdots$
ρ_M

Model parameters are then ordered into a vector by column from top to bottom elements,

$$m = \begin{bmatrix} \rho_1 \\ \vdots \\ \rho_M \end{bmatrix}_{M\times 1} \tag{3.9}$$

where M is the number of model parameters which is equal to the total number of discretized model blocks.

The inverse covariance matrix can be expressed as

$$C_d^{-1} = W_d^{\mathrm{T}} W_d, \tag{3.10}$$

where

$$W_d = \begin{bmatrix} 1/\epsilon_1 & & & \\ & 1/\epsilon_2 & & \\ & & \ddots & \\ & & & 1/\epsilon_N \end{bmatrix}_{N\times N}. \tag{3.11}$$

3.2.2 Model functional

$$\Phi_m = \chi_m^2 - \chi_{m^*}^2, \tag{3.12}$$

$$\chi_m^2 = \sum_{i=1}^{M} (m_{i+1} - m_i)^2. \tag{3.13}$$

Equation (3.13) can be expressed in matrix form as,

$$\chi_m^2 = (m_{k+1} - m_0)^{\mathrm{T}} C_m^{-1} (m_{k+1} - m_0),$$

where m_0 is the reference prior model, C_m^{-1} is the model covariance.

The model roughness or the inverse of the model covariance (C_m^{-1}) operator is introduced in Degroot-Hedlin & Constable (1990) as,

$$C_m^{-1} = \Delta_z^{\mathrm{T}} \Delta_z, \tag{3.14}$$

where

$$\Delta_z = \begin{bmatrix} 0 & & & & & \\ -1 & 1 & & & & \\ & -1 & 1 & & & \\ & & \ddots & \ddots & & \\ & & & -1 & 1 \end{bmatrix}_{M \times M}. \tag{3.15}$$

3.2.3 Minimization of an Objective Function

For Occam's inversion, the objective function can be expressed according to the given data functional and model functional as

$$W(\lambda, m) = (m - m_0)^{\mathrm{T}} C_m^{-1} (m - m_0) + \lambda^{-1} \left[(d - \mathrm{F}[m])^{\mathrm{T}} C_d^{-1} (d - \mathrm{F}[m]) - \chi_{d^*}^2 \right], \tag{3.16}$$

where $\chi_{d^*}^2$ is the desired level of misfit.

We use a Taylor's series expansion to linearize $\mathrm{F}[m]$ as

$$\mathrm{F}[m + \Delta m] = \mathrm{F}[m] + \frac{\partial \mathrm{F}[m]}{\partial m} \Delta m. \tag{3.17}$$

Since $m_{k+1} = m_k + \Delta m$, equation (3.2.3) can be written in iterative form,

$$\mathrm{F}[m_{k+1}] = \mathrm{F}[m_k] + J_k (m_{k+1} - m_k), \tag{3.18}$$

where k denotes the iteration number,
m_{k+1} represents the model at the next iteration,
the first derivative J_k is the Jacobian or sensitivity calculated at iteration k and

$$J_k \equiv \frac{\partial \mathrm{F}[m]}{\partial m}.$$

We calculate the Jacobian using forward difference method as

$$J_k = \begin{bmatrix} \frac{F[m+\rho_1]_1 - F[m]_1}{\rho_1} & \cdots & \frac{F[m+\rho_M]_1 - F[m]_1}{\rho_N} \\ \vdots & \ddots & \vdots \\ \frac{F[m+\rho_1]_{2N} - F[m]_{2N}}{\rho_1} & \cdots & \frac{F[m+\rho_M]_{2N} - F[m]_{2N}}{\rho_N} \end{bmatrix}_{2N \times M}.$$

Substituting equation (3.18) into equation (3.16), we get the objective function in iterative form,

$$W_\lambda = (m_{k+1}-m_0)^{\mathrm{T}} C_m^{-1}(m_{k+1}-m_0) + \lambda^{-1}\left[\left(d-\mathrm{F}[m_k]-J_k(m_{k+1}-m_k)\right)^{\mathrm{T}} C_d^{-1}\left(d-\mathrm{F}[m_k]-J_k(m_{k+1}-m_k)\right)-\chi_{d^*}^2\right]. \tag{3.19}$$

To incorporate the prior model m_0 into the inversion, we replace as

$$m_{k+1}-m_k = (m_{k+1}-m_0)-(m_k-m_0),$$

and substitute into equation (3.19). The objective function becomes

$$W_\lambda = (m_{k+1}-m_0)^{\mathrm{T}} C_m^{-1}(m_{k+1}-m_0) + \lambda^{-1}\left[\left(\hat{d}-J_k(m_{k+1}-m_0)\right)^{\mathrm{T}} C_d^{-1}\left(\hat{d}-J_k(m_{k+1}-m_0)\right)-\chi_{d^*}^2\right], \tag{3.20}$$

where $\hat{d} = d-\mathrm{F}[m_k]+J_k(m_k-m_0)$.

In order to find the m_{k+1} that minimizes the objective function, we differentiate equation (3.20) with respect to m_{k+1} at the stationary point,

$$\frac{\partial W_\lambda}{\partial m_{k+1}} = 0. \tag{3.21}$$

Hence, the expression of the iterative sequence is (see Vachiratienchai, 2007; Boonchaisuk, 2007)

$$m_{k+1} = (\lambda C_m^{-1}+\Gamma_k^m)^{-1} J_k^T C_d^{-1}\hat{d} + m_0, \tag{3.22}$$

where $\Gamma_k^m = J_k^T C_d^{-1} J_k$.

3.2.4 Pseudo code for Jacobian

Import F$[m_k]$, frequencies, resistivities, and thicknesses of each layers, and dm

for all layers

  Add dm with each layer

  Calculate F$[m_k+dm]$

end

Calculate Jacobian $= \frac{\mathrm{F}[m_k+dm]-\mathrm{F}[m_k]}{dm}$

3.2.5 Pseudo code for Occam's inversion

Import synthetic data or observed data

Assign error of each data to get C_d^{-1}

Assign initial model or m_0

Assign C_m^{-1}

Assign m_1 using $m_k = m_0$

for 2^{nd} iteration to the iteration that m_{k+1} satisfy some condition e.g. data misfit

  for $\log_{10}(\lambda) = 0$ to 6

    Choose the λ that give the lowest data misfit

  end

Calculate $m_{k+1} = (\lambda C_m^{-1} + \Gamma_k^m)^{-1} J_k^T C_d^{-1} \hat{d} + m_0$

end

3.3 Occam's inversion with Spatial Constraint

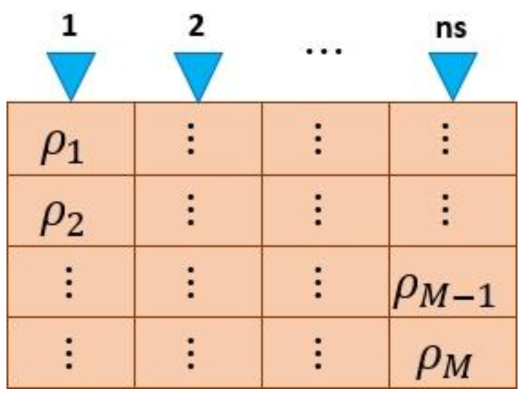

Figure 3.2: 2-D Earth Model

Both forward response vector and the model vector of each site station, we connect the vector until the last vector as

$$F[m] = \begin{bmatrix} \rho_{a1_1} \\ \vdots \\ \rho_{aN_1} \\ \phi_{1_1} \\ \vdots \\ \phi_{N_1} \\ \rho_{a1_2} \\ \vdots \\ \rho_{aN_2} \\ \phi_{1_2} \\ \vdots \\ \phi_{N_2} \\ \vdots \\ \rho_{a1_{ns}} \\ \vdots \\ \rho_{aN_{ns}} \\ \phi_{1_{ns}} \\ \vdots \\ \phi_{N_{ns}} \end{bmatrix}_{(2N\times ns)\times 1}, \tag{3.23}$$

and

$$m = \begin{bmatrix} \rho_1 \\ \rho_2 \\ \vdots \\ \rho_M \end{bmatrix}_{M\times 1}, \tag{3.24}$$

where *ns* is the number of station.
We connect all Jacobian of each station to be band matrix in each *k* iteration as

$$J = \begin{bmatrix} J_{k_1} & \cdots & & \\ \vdots & J_{k_2} & & \vdots \\ & & \ddots & \\ & \cdots & & J_{k_{ns}} \end{bmatrix}_{(2N\times ns)\times M}.$$

We change to use the model roughness or the inverse of the model covariance (C_m^{-1}) operator is introduced in Degroot-Hedlin & Constable (1990) as,

$$C_m^{-1} = \Delta x^T \Delta x + \Delta z^T \Delta z \tag{3.25}$$

where Δ_z is the same as the equation (3.15)

$$\Delta_x = \begin{bmatrix} -1 & & & & 1 & & & \\ & -1 & & & & 1 & & \\ & & \ddots & & & & \ddots & \\ & & & -1 & & & & 1 \\ & & & 0 & & & & \end{bmatrix}_{M \times M}, \tag{3.26}$$

where 0 is an $M_z \times M$ zeros matrix,
and there are $M_z - 1$ zeros between the entries in each row of Δx.

3.3.1 Pseudo code for Occam's inversion with spatial constraint

Import observed data

Connect data of all station to be one vertical vector

Assign error of each data to get C_d^{-1}

Assign initial model or m_0

Assign C_m^{-1} in 2-D

Assign m_1 using $m_k = m_0$

for 2nd iteration to the iteration that m_{k+1} satisfy some condition e.g. data misfit

  for $\log_{10}(\lambda) = 0$ to 6

    Choose the λ that give the lowest data misfit

  end

Calculate $m_{k+1} = (\lambda C_m^{-1} + \Gamma_k^m)^{-1} J_k^T C_d^{-1} \hat{d} + m_0$

end

CHAPTER IV
RESULTS AND DISCUSSION

4.1 Forward Modeling

I assign resistivity in each layer to check the results of the forward modeling by showing in apparent resistivity and phase in figure 4.1-4.5.

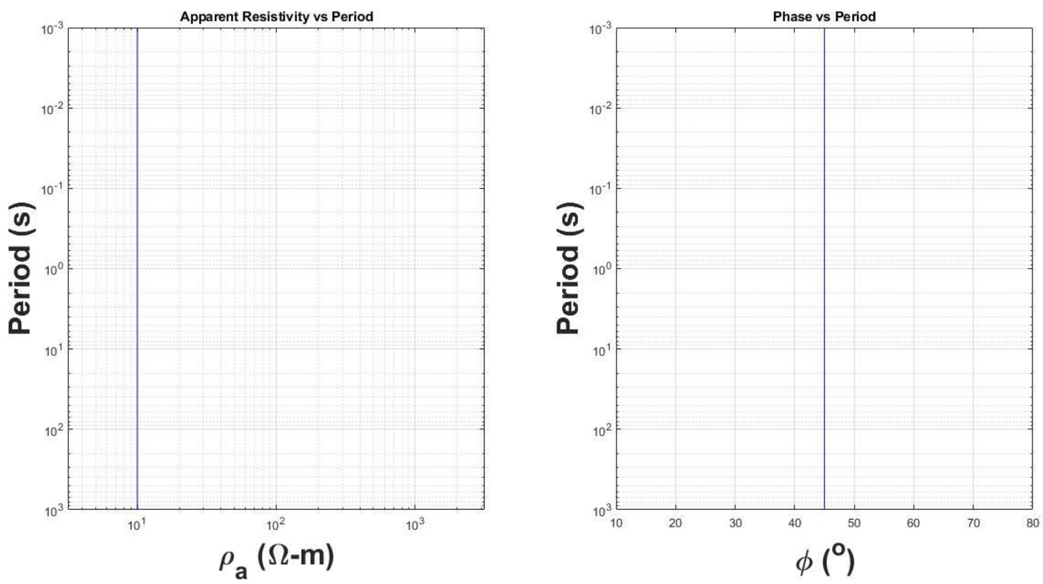

Figure 4.1: graphs of apparent resistivity vs period and phase vs period in 3-layered resistivity earth model [10; 10; 10].

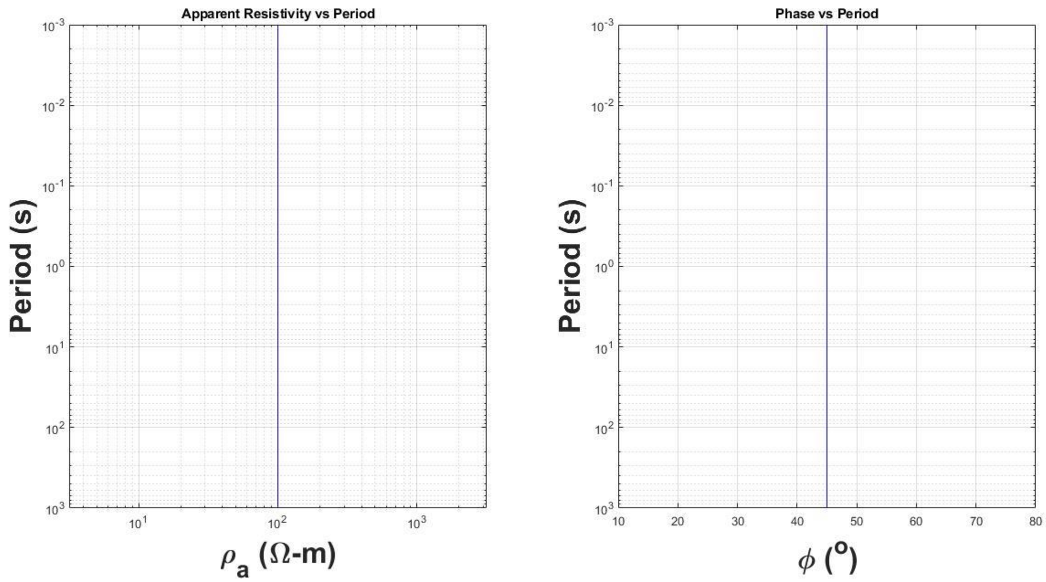

Figure 4.2: graphs of apparent resistivity vs period and phase vs period in 3-layered resistivity earth model [100; 100; 100].

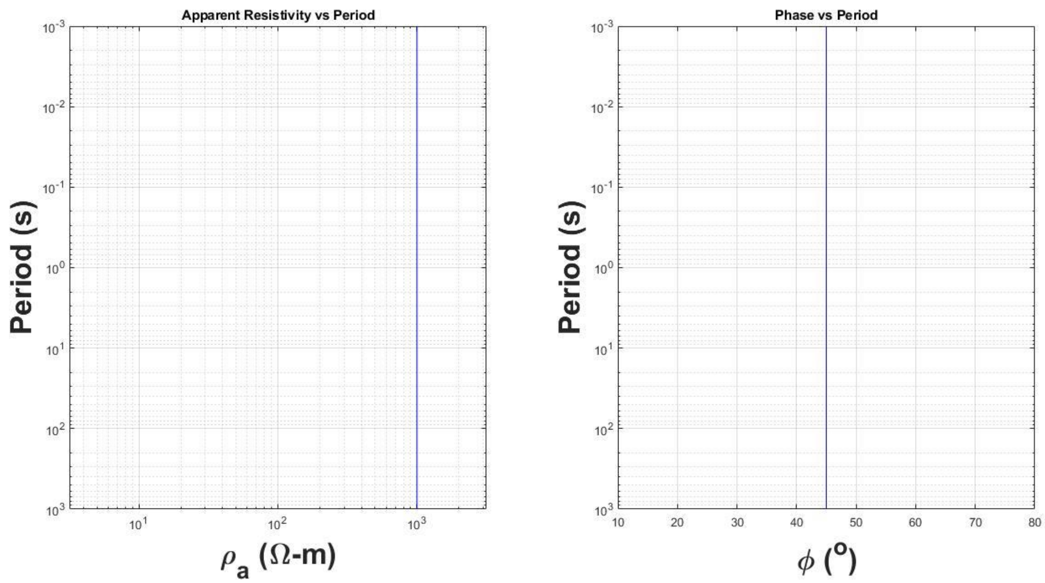

Figure 4.3: graphs of apparent resistivity vs period and phase vs period in 3-layered resistivity earth model [1000; 1000; 1000].

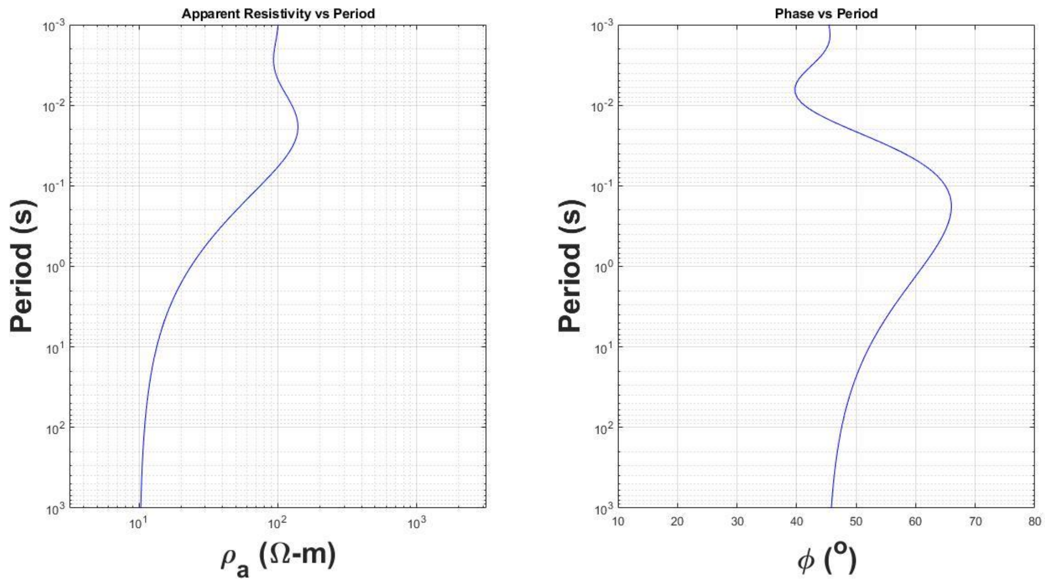

Figure 4.4: graphs of apparent resistivity vs period and phase vs period in 3-layered resistivity earth model [100; 1000; 10].

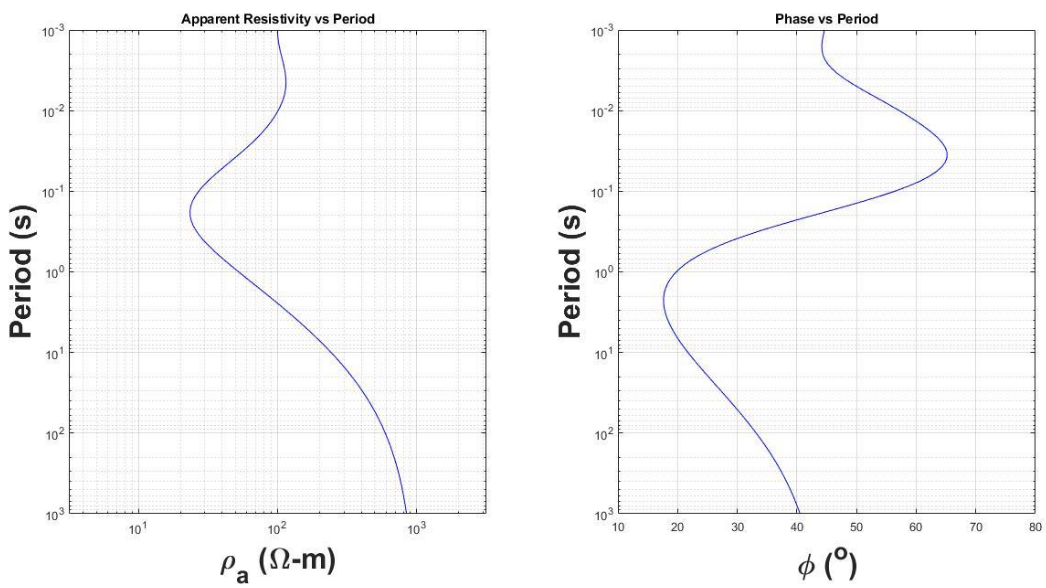

Figure 4.5: graphs of apparent resistivity vs period and phase vs period in 3-layered resistivity earth model [100; 10; 1000].

4.2 Inversion

I show the results using Occam's inversion and compare to synthetic data and model in figure 4.6-4.7, which they give the mean relative error that pretty satisfies.

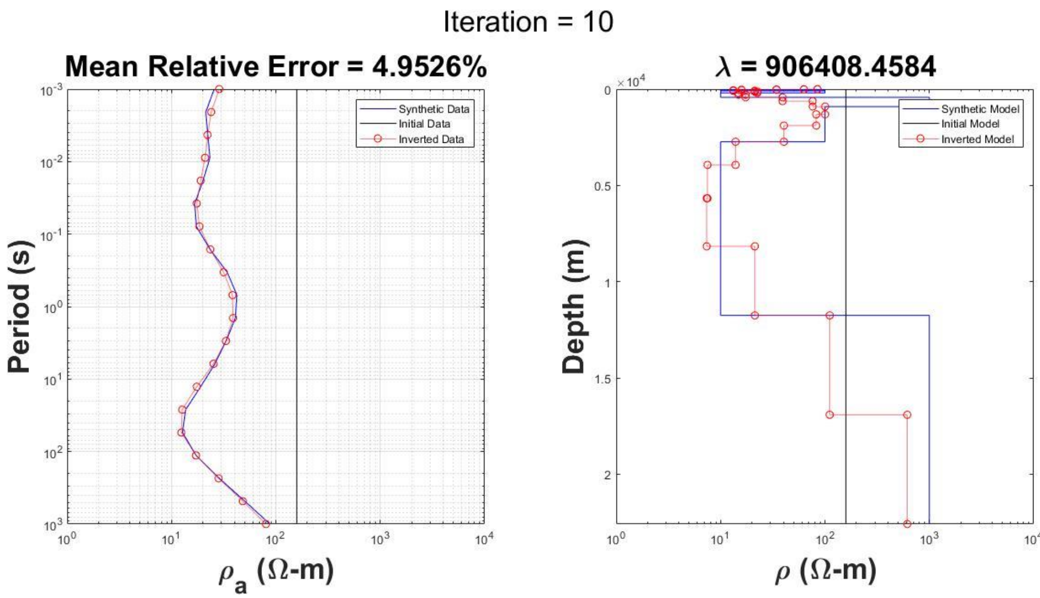

Figure 4.6: graphs of apparent resistivity vs period and resistivity vs depth in 20-layered resistivity earth model [2; 2; 2; 1; 1; 2; 2; 1; 1; 3; 3; 2; 2; 2; 1; 1; 1; 1; 3; 3] in log-sacle.

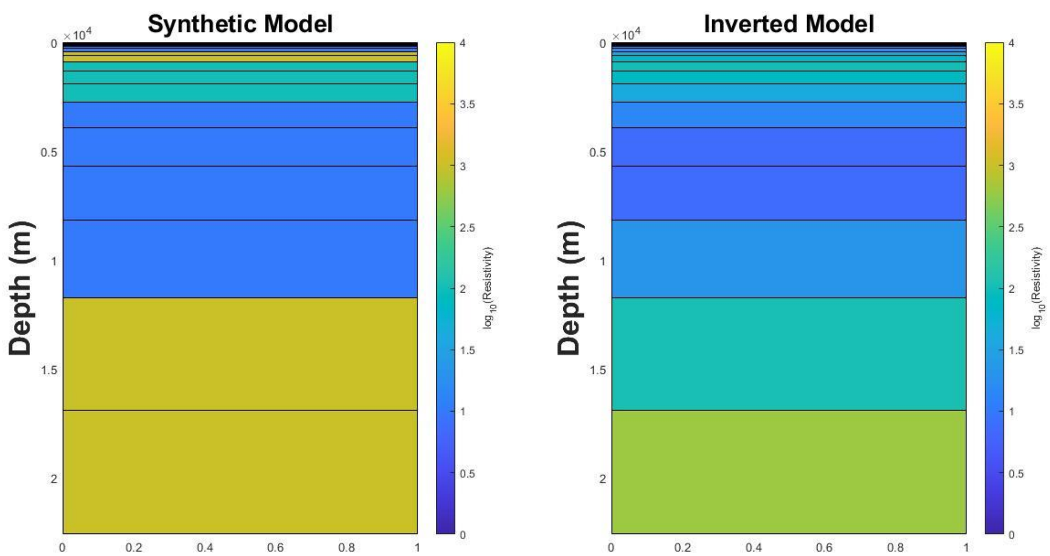

Figure 4.7: Comparison between synthetic resistivity model and inverted resistivity model in 20-layered resistivity earth model [2; 2; 2; 1; 1; 2; 2; 1; 1; 3; 3; 2; 2; 2; 1; 1; 1; 1; 3; 3] in log-sacle.

4.3 Inversion with Spatial Constraint

I use the same data with the previous inversion results but add 1 more station to be 2 stations and run inversion with constraint in figure 4.8-4.11.

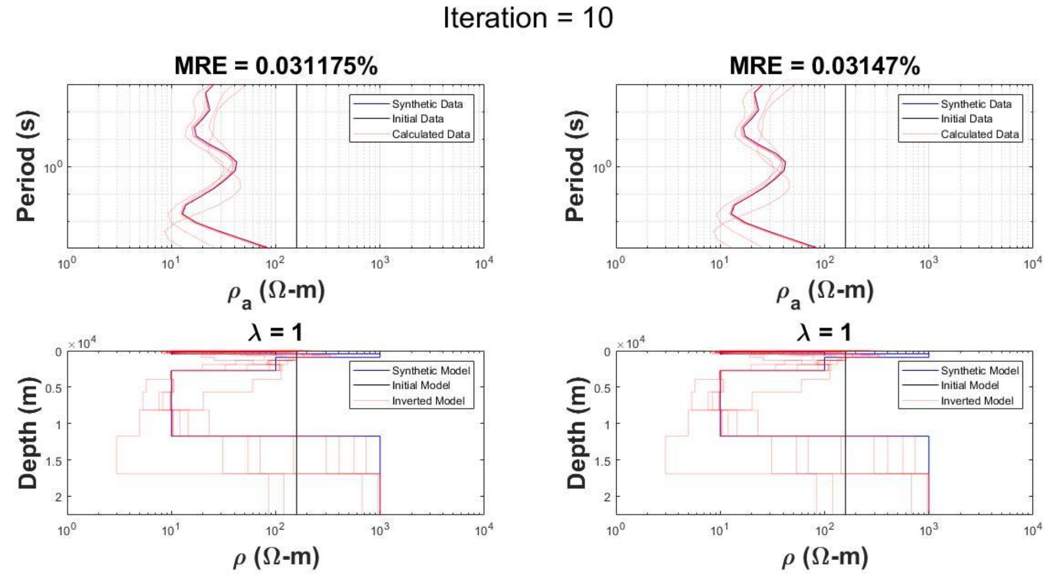

Figure 4.8: graphs of apparent resistivity vs period and resistivity vs depth in 20-layered resistivity earth model [2; 2; 2; 1; 1; 2; 2; 1; 1; 3; 3; 2; 2; 2; 1; 1; 1; 1; 3; 3] in log-sacle of both stations in 1-10 iteration.

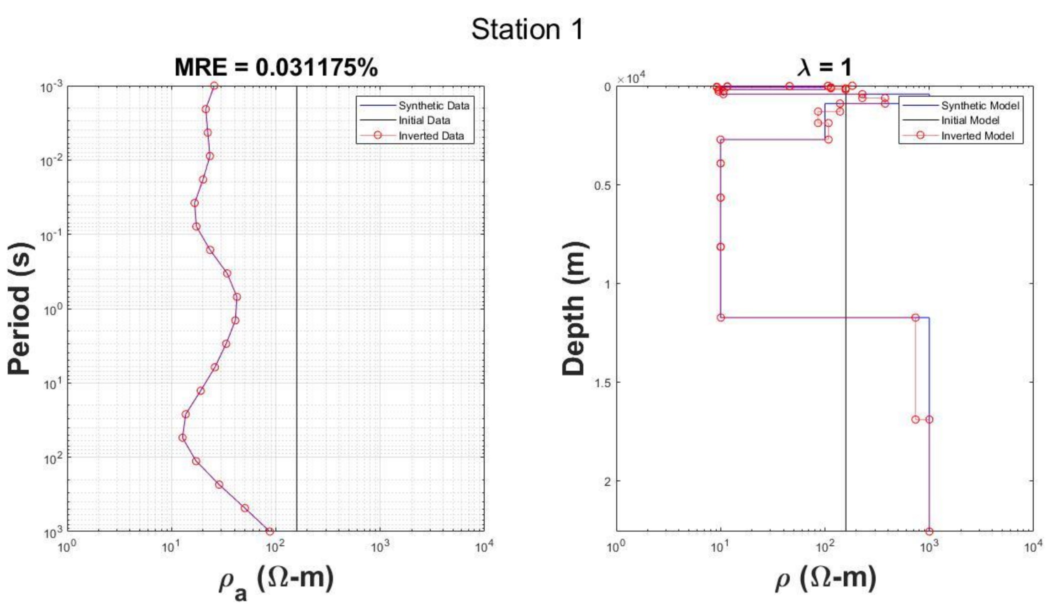

Figure 4.9: graphs of apparent resistivity vs period and resistivity vs depth in 20-layered resistivity earth model [2; 2; 2; 1; 1; 2; 2; 1; 1; 3; 3; 2; 2; 2; 1; 1; 1; 1; 3; 3] in log-sacle in station 1.

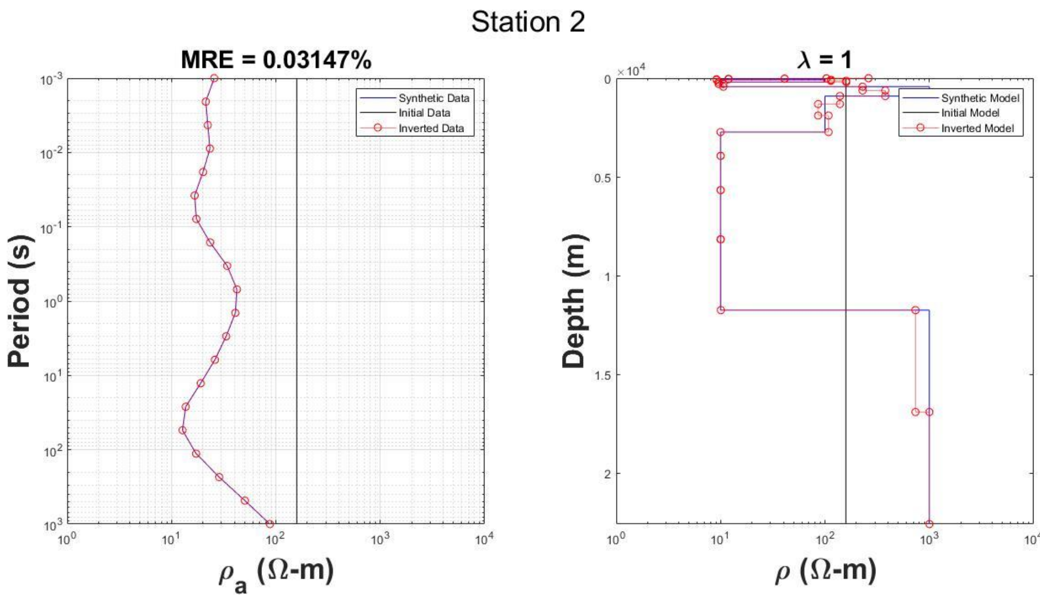

Figure 4.10: graphs of apparent resistivity vs period and resistivity vs depth in 20-layered resistivity earth model [2; 2; 2; 1; 1; 2; 2; 1; 1; 3; 3; 2; 2; 2; 1; 1; 1; 1; 3; 3] in log-sacle in station 2.

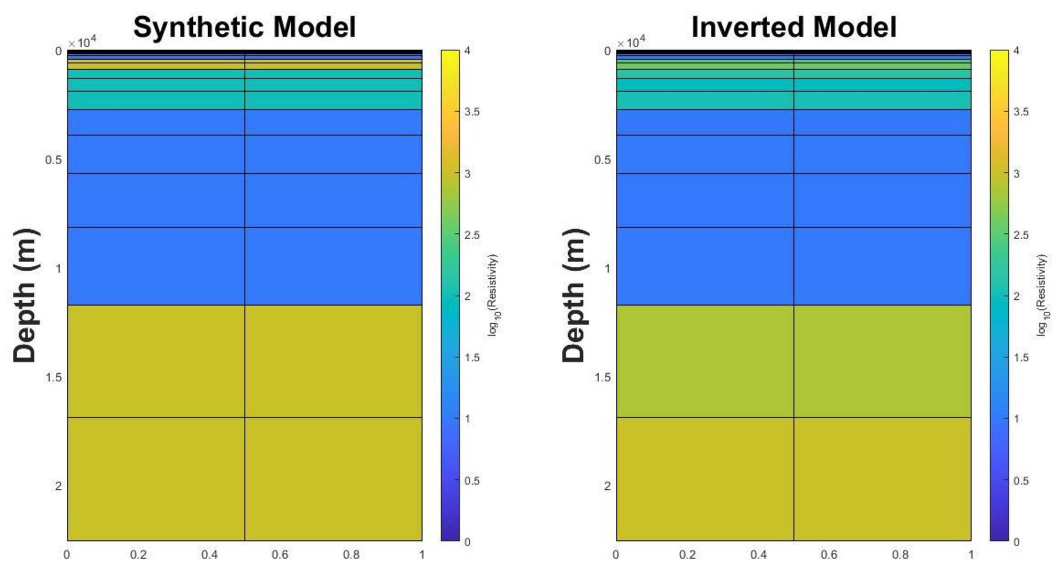

Figure 4.11: Comparison between synthetic resistivity model and inverted resistivity model in 20-layered resistivity earth model [2; 2; 2; 1; 1; 2; 2; 1; 1; 3; 3; 2; 2; 2; 1; 1; 1; 1; 3; 3] in log-sacle with constraint.

4.4 Inversion with Spatial Constraint in Real Data; 3-D resistivity model from Mae Chan geothermal system (P. Amatyakul et al., 2015)

Finally, I try to test my inversion with real data from from 3-D resistivity model from Mae Chan geothermal system (P. Amatyakul et al., 2015) in figure 4.12-4.14.

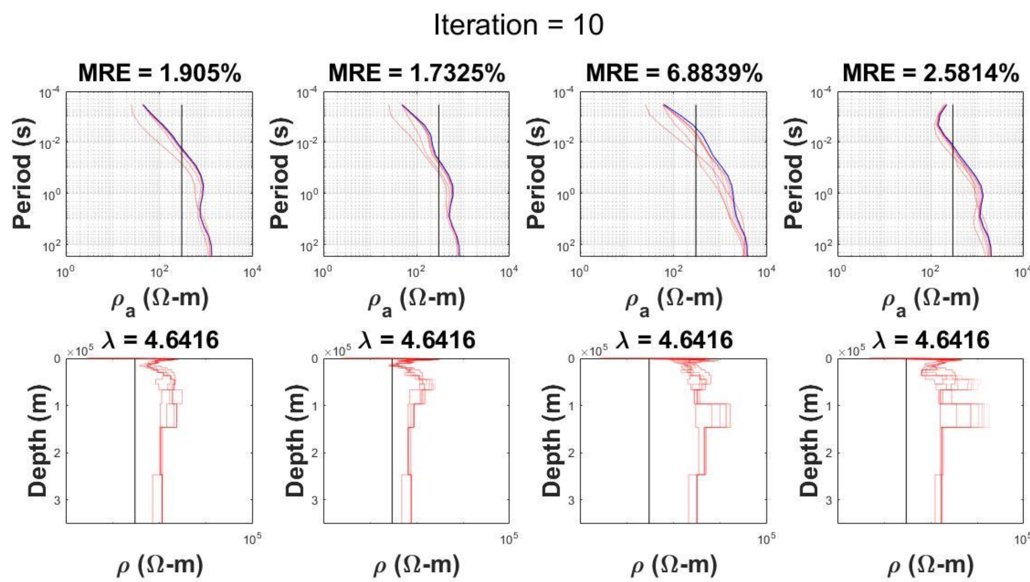

Figure 4.12: graphs of apparent resistivity vs period and resistivity vs depth of 4 in 34 station using data from 3-D resistivity model from Mae Chan geothermal system (P. Amatyakul et al., 2015)

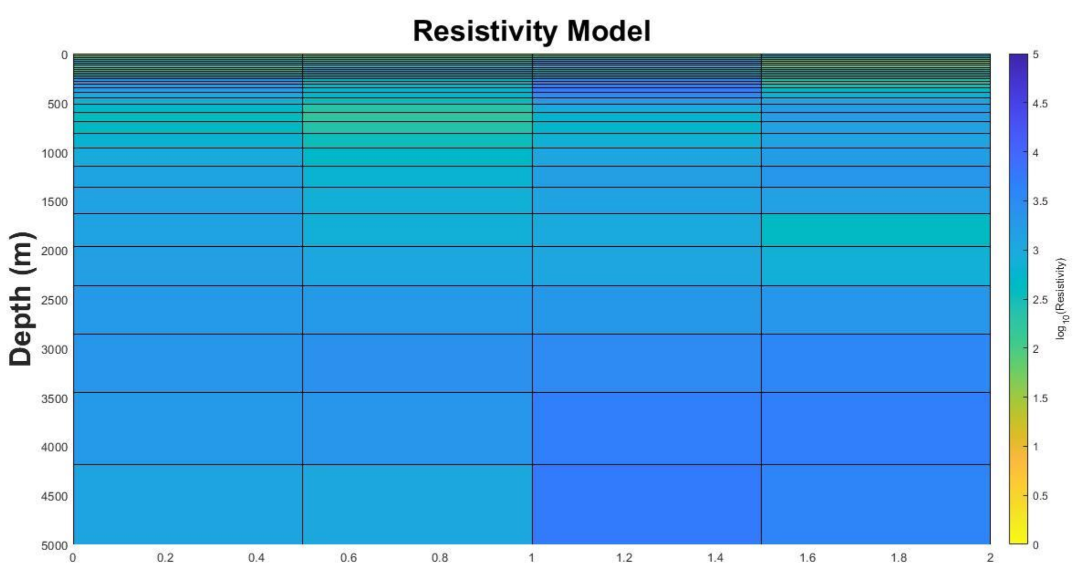

Figure 4.13: Inverted resistivity model of 4 in 34 station using data from 3-D resistivity model from Mae Chan geothermal system (P. Amatyakul et al., 2015)

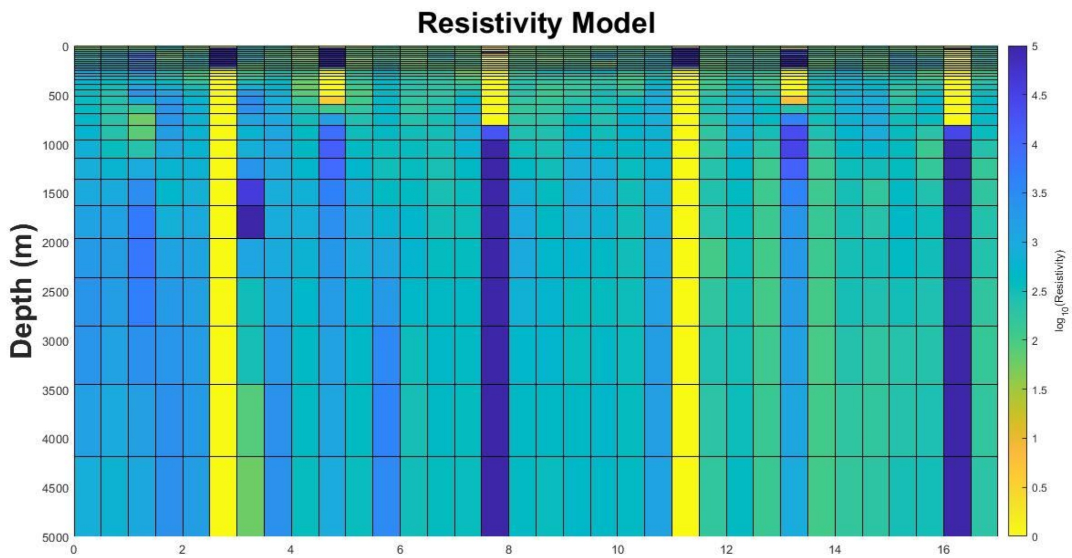

Figure 4.14: Inverted resistivity model of all 34 stations using data from 3-D resistivity model from Mae Chan geothermal system (P. Amatyakul et al., 2015)

4.5 Discussion

From Fig. 4.1-4.3, the apparent resistivity trend is straight line at the assigned resistivity value in each model because the resistivity doesn't change. Likewise, the phase trend is also straight line at 45 degree because the apparent resistivity doesn't change. Then I assign model that has different resistivity in each layer in Fig. 4.4-4.5, the apparent resistivity gradually increases or decreases following assigned resistivity, but the phase will increase if the apparent resistivity decrease, the phase will decrease if the apparent resistivity increase and the phase will constant if the apparent resistivity doesn't change.

From Fig. 4.6-4.11, a synthetic test in a given resistance condition, the results are quite effective. In the case of a few stations are good but trying to test the data in many stations, there are lots of errors and the response to the model is not smooth enough.

CHAPTER V
SUMMARY

This project aims to 1-D MT inversion with spatial constraint. The calculation starts from the forward modeling applying boundary conditions for 1-D layered earth, then these conditions result in a recursive formula relating impedance of two consecutive layers. The apparent resistivity and phase are calculated in various frequencies (periods) and use for Occam’s inversion. Adding the spatial constraint by changing the model roughness to 2-D instead. The inversion results approach to the synthetic results, but using real data is not effective in many stations yet. The future works are to develop coding for a better result and compare to the real data from 3-D resistivity model from Mae Chan geothermal system (P. Amatyakul et al., 2015).

REFERENCES

Charles Muturia Lichoro. *Comparison of 1-D, 2-D and 3-D Inversion Approaches of Interpreting Electromagnetic Data of Silali Geothermal Area*. Proceedings World Geothermal Congress 2015.

Esben Auken, Anders V. Christiansen, Bo H. Jacobsen, Nikolaj Foged and Kurt I. Sørensen. *Piecewise 1D laterally constrained inversion of resistivity data*. Geophysical Prospecting, 2005, 53, 497–506.

Fernando Aca´cio Monteiro Santos, John Triantafilis, and Kira Bruzgulis. *A spatially constrained 1D inversion algorithm for quasi-3D conductivity imaging: Application to DUALEM-421 data collected in a riverine plain*. GEOPHYSICS, VOL. 76, NO. 2 (MARCH-APRIL 2011); P. B43–B53, 11 FIGS.

G. D. Naidu, *Deep Crustal Structure of the Son–Narmada–Tapti Lineament, Central India*, Springer Theses.

Gianluca Fiandaca, Esben Auken, Anders Vest Christiansen, and Aurélie Gazoty. *Time-domain-induced polarization: Full-decay forward modeling and 1D laterally constrained inversion of Cole-Cole parameters*. GEOPHYSICS, VOL. 77, NO. 3 (MAY-JUNE 2012); P. E213–E225, 12 FIGS., 1 TABLE.

Puwis Amatyakul, Tawat Rung-Arunwan, Weerachai Siripunvaraporn. *A pilot magnetotelluric survey for geothermal exploration in Mae Chan region, northern Thailand*. Geothermics 55 (2015) 31–38.

Songkhun Boonchaisuk, Weerachai Siripunvaraporn, Yasuo Ogawa. *Evidence for middle Triassic to Miocene dual subduction zones beneath the Shan–Thai terrane, western Thailand from magnetotelluric data.* Gondwana Research 23 (2013) 1607–1616.

Weerachai Siripunvaraporna, and Gary Egbert. *WSINV3DMT: Vertical magnetic field transfer function inversion and parallel implementation.* Physics of the Earth and Planetary Interiors 173 (2009) 317–329.

Weerachai Siripunvaraporna, Gary Egbert, Yongwimon Lenbury, and Makoto Uyeshima. *Three-dimensional magnetotelluric inversion: data-space method*. Physics of the Earth and Planetary Interiors 150 (2005) 3–14.